SOIL, 5, 49–62, 2019
https://doi.org/10.5194/soil-5-49-2019


SOIL Open Access EGU

# Application of a laser-based spectrometer for continuous in situ measurements of stable isotopes of soil $CO_2$ in calcareous and acidic soils

**Jobin Joseph[1], Christoph Külls[2], Matthias Arend[3], Marcus Schaub[1], Frank Hagedorn[1], Arthur Gessler[1], and Markus Weiler[4]**

[1]Swiss Federal Institute for Forest, Snow and Landscape Research WSL, Zürcherstrasse 111, 8903 Birmensdorf, Switzerland
[2]Laboratory for Hydrology and International Water Management, University of Applied Sciences, Lübeck, Germany
[3]Physiological Plant Ecology (PPE), Faculty of Integrative Biology, University of Basel, Basel, Switzerland
[4]Faculty of Environment and Natural resources, University of Freiburg, Freiburg, Germany

**Correspondence:** Jobin Joseph (jobin.joseph@wsl.ch)

Received: 27 April 2018 – Discussion started: 30 May 2018
Revised: 14 January 2019 – Accepted: 18 January 2019 – Published: 31 January 2019

**Abstract.** The short-term dynamics of carbon and water fluxes across the soil–plant–atmosphere continuum are still not fully understood. One important constraint is the lack of methodologies that enable simultaneous measurements of soil $CO_2$ concentration and respective isotopic composition at a high temporal resolution for longer periods of time. $\delta^{13}C$ of soil $CO_2$ can be used to derive information on the origin and physiological history of carbon, and $\delta^{18}O$ in soil $CO_2$ aids in inferring the interaction between $CO_2$ and soil water. We established a real-time method for measuring soil $CO_2$ concentration, $\delta^{13}C$ and $\delta^{18}O$ values across a soil profile at higher temporal resolutions (0.05–0.1 Hz) using an off-axis integrated cavity output spectroscopy (OA-ICOS). We also developed a calibration method correcting for the sensitivity of the device against concentration-dependent shifts in $\delta^{13}C$ and $\delta^{18}O$ values under highly varying $CO_2$ concentration. The deviations of measured data were modelled, and a mathematical correction model was developed and applied for correcting the shift. By coupling an OA-ICOS with hydrophobic but gas-permeable membranes placed at different depths in acidic and calcareous soils, we investigated the contribution of abiotic and biotic components to total soil $CO_2$ release. We found that in the calcareous Gleysol, $CO_2$ originating from carbonate dissolution contributed to the total soil $CO_2$ concentration at detectable degrees, potentially due to $CO_2$ evasion from groundwater. The $^{13}C$-$CO_2$ of topsoil at the calcareous soil site was found reflect $\delta^{13}C$ values of atmospheric $CO_2$, and the $\delta^{13}C$ of topsoil $CO_2$ at the acidic soil site was representative of the biological respiratory processes. $\delta^{18}O$ values of $CO_2$ in both sites reflected the $\delta^{18}O$ of soil water across most of the depth profile, except for the 80 cm depth at the calcareous site where a relative enrichment in $^{18}O$ was observed.

## 1 Introduction

Global fluxes of $CO_2$ and $H_2O$ are two major driving forces controlling earth's climatic systems. To understand the prevailing climatic conditions and predict climate change, accurate monitoring and modelling of these fluxes are essential (Barthel et al., 2014; Harwood et al., 1999; Schär et al., 2004). Soil respiration, the $CO_2$ flux released from the soil surface to the atmosphere as a result of microbial and root respiration (heterotrophic and autotrophic), is the second largest terrestrial carbon flux (Bond-Lamberty and Thomson, 2010). The long-term dynamics of $CO_2$ release on a seasonal scale are reasonably well understood (Satakhun et al., 2013), whereas less information on $CO_2$ dynamics and iso-

topic composition is available for short-term variations on a diurnal scale (Werner and Gessler, 2011). The lack of a proper understanding of the diurnal fluctuations in soil $CO_2$ release might introduce uncertainty in estimating the soil carbon budget and the $CO_2$ fluxes to the atmosphere. The isotopic composition of soil $CO_2$ and its diel fluctuation can be a critical parameter for the partitioning of ecosystem gas exchange into its components (Bowling et al., 2003; Mortazavi et al., 2004) and for disentangling plant and ecosystem processes (Werner and Gessler, 2011). By assessing the $\delta^{13}C$ of soil $CO_2$, it is possible to identify the source for $CO_2$ (Kuzyakov, 2006) and the coupling between photosynthesis and soil respiration when taking into account post-photosynthetic isotope fractionation (Werner et al., 2012; Wingate et al., 2010). $\delta^{13}C$ soil $CO_2$ reflects, however, not only microbial and root respiration but also abiotic sources from carbonate weathering (Schindlbacher et al., 2015).

Soil water imprints its $\delta^{18}O$ signature on soil $CO_2$ as a result of isotope exchange between $H_2O$ and $CO_2$ (aqueous). The oxygen isotopic exchange between $CO_2$ and soil water is catalysed by microbial carbonic anhydrase (Sperber et al., 2015; Wingate et al., 2009). Thus, soil $CO_2$ can give information on the isotopic composition of both soil water resources and carbon sources. The oxygen isotope composition of plant-derived $CO_2$ is both a tracer of photosynthetic and respiratory $CO_2$ and gives additional quantitative information on the water cycle in terrestrial ecosystems (Francey and Tans, 1987). To better interpret the $\delta^{13}C$ and $\delta^{18}O$ signals of atmospheric $CO_2$, the isotopic composition and its variability in the different sources need to be better understood (Werner et al., 2012; Wingate et al., 2010).

The conventional method for estimating the $\delta^{13}C$ and $\delta^{18}O$ of soil $CO_2$ efflux is by using two end-member mixing models of atmospheric $CO_2$ and $CO_2$ produced in the soil (Keeling, 1958). The conventional methods for sampling soil produced $CO_2$ are chamber-based (Bertolini et al., 2006; Torn et al., 2003), "mini-tower" (Kayler et al., 2010; Mortazavi et al., 2004), and soil-gas-well-based (Breecker and Sharp, 2008; Oerter and Amundson, 2016) methods. In conventional methods, air sampling is done at specific time intervals, and $\delta^{13}C$ and $\delta^{18}O$ are analysed using isotope ratio mass spectrometry (IRMS; Ohlsson et al., 2005). Such offline methods have several disadvantages, like high sampling costs, excessive time consumption for sampling and analysis, and increased sampling error and low temporal resolution. Kammer et al. (2011), showed how error prone the conventional methods could be while calculating $\delta^{13}C$ and $\delta^{18}O$ (up to several per mil when using chamber and mini-tower-based methods; Kammer et al., 2011). In chamber-based systems, non-steady-state conditions may arise within the chamber due to increased $CO_2$ concentrations, which in turn hinders the diffusion of $^{12}CO_2$ more strongly than that of heavier $^{13}CO_2$ (Risk and Kellman, 2008). Moreover, it has been found that $\delta^{18}O$ of the $CO_2$ inside a chamber is significantly influenced by the $\delta^{18}O$ of the surface soil water, as an equilibrium isotopic exchange happens during the upward diffusive movement of soil $CO_2$ (Mortazavi et al., 2004). The advent of laser-based isotope spectroscopy has enabled cost-effective, simple, and high precision real-time measurements of $\delta^{13}C$ and $\delta^{18}O$ in $CO_2$ (Kammer et al., 2011; Kerstel and Gianfrani, 2008). This technique opened up new possibilities for faster and reliable measurements of stable isotopes in situ, based on the principle of light absorption, using laser beams of distinct wavelengths in the near- and mid-infrared range (Bowling et al., 2003). Recently, several high-frequency online measurements of $\delta^{13}C$ and $\delta^{18}O$, of soil $CO_2$ and $^2H$, and of the $^{18}O$ of soil water vapour across soil depth profiles were reported by coupling either hydrophobic but gas-permeable membranes (installed at different depths in soil) or automated chamber systems with laser spectrometers (Bowling et al., 2015; Jochheim et al., 2018; Stumpp et al., 2018). Such approaches enable detection of vertical concentration profiles, temporal dynamics of soil $CO_2$ concentration, and the isotopic signature of soil $CO_2$ across different soil layers, thus aiding in identifying and quantifying various sources of $CO_2$ across the depth profile.

In 1988, O'Keefe and Decon introduced cavity ring-down spectroscopy (CRDS) for measuring the isotopic ratio of different gaseous species based on laser spectrometry (O'Keefe and Deacon, 1988). With the laser-based spectrometry techniques, measuring sensitivities up to parts per trillion (ppt) concentrations is achieved (von Basum et al., 2004; Peltola et al., 2012). In CRDS, the rate of change in the absorbed radiation of the laser light that is temporarily "trapped" within a highly reflective optical cavity is determined. This is achieved using resonant coupling of a laser beam to the optical cavity and active locking of laser frequency to cavity length (Parameswaran et al., 2009). Another well-established technique similar to CRDS is off-axis integrated cavity output spectroscopy (OA-ICOS). It is based on directing narrowband and continuous-wave lasers in an off-axis configuration to the optical cavity (Baer et al., 2002).

Even though OA-ICOS can measure concentration and isotope signature of various gaseous species at a high temporal resolution, we found pronounced deviations in $\delta^{13}C$ and $\delta^{18}O$ measurements from the absolute values when measured under changing $CO_2$ concentrations. So far, to our knowledge, no study detailing the calibration process of OA-ICOS $CO_2$ analysers correcting for fluctuations of both $\delta^{13}C$ and $\delta^{18}O$ values under varying $CO_2$ concentrations has been made available. Most of the OA-ICOS $CO_2$ analysers are built for working under stable $CO_2$ concentrations, so periodical calibration against in-house gas standards at a particular concentration is sufficient. However, as there are pronounced gradients in $CO_2$ levels in soils (Maier and Schack-Kirchner, 2014), $CO_2$-concentration-dependent shifts in measured isotopic values have to be addressed and corrected. Such calibration is, however, also relevant for any other OA-ICOS application with varying levels of $CO_2$ (e.g. in chamber measurements). Hence the first part of this work comprises the

establishment of a calibration method for OA-ICOS. The second part describes a method for online measurement of $CO_2$ concentrations and stable carbon and oxygen isotope composition of $CO_2$ in different soil depths by coupling OA-ICOS with gas-permeable hydrophobic tubes (membrane tubes, Accurel®). The use of these tubes for measuring soil $CO_2$ concentration (Gut et al., 1998) and the $\delta^{13}C$ of soil $CO_2$ (Parent et al., 2013) has already been established, but the coupling to an OA-ICOS system has not been performed, yet.

We evaluated our measurement system by assessing and comparing the concentration of the $\delta^{13}C$ and $\delta^{18}O$ of soil $CO_2$ for a calcareous and an acidic soil system. The primary foci of this study are to (1) introduce OA-ICOS in online soil $CO_2$ concentration and isotopic measurements, (2) calibrate the OA-ICOS to render it usable for isotopic analysis carried out under varying $CO_2$ concentrations, and (3) analyse the dynamics of $\delta^{13}C$ and $\delta^{18}O$ of soil $CO_2$ at different soil depths in different soil types at a higher temporal resolution.

## 2 Materials and methods

### 2.1 Instrumentation

The concentration of $\delta^{13}C$ and $\delta^{18}O$ values of $CO_2$ were measured with an OA-ICOS, as described in detail by Baer et al. (2002) and Jost et al. (2006). In this study, we used an OA-ICOS, (LGR CCIA 36-d) manufactured by Los Gatos Research Ltd in San Francisco, USA. The LGR CCIA 36-d measures $CO_2$ concentration and $\delta^{13}C$ and $\delta^{18}O$ values at a frequency up to 1 Hz. The operational $CO_2$ concentration range was 400 to 25 000 ppm. The operating temperature range was +10–+35 °C, and the sample temperature range (gas temperature) was between −20 and 50 °C. The recommended inlet pressure was < 0.0689 MPa. The multiport inlet unit (MIU), an optional design that comes along with LGR CCIA 36-d, had a manifold of eight digitally controlled inlet ports and one outlet port. It presented the user with an option of measuring eight different $CO_2$ samples at the desired time interval. Three standard gases with distinct $\delta^{13}C$ and $\delta^{18}O$ values were used for calibration in this study (see Table S1 in the Supplement). The standard gases used in this study were analysed for absolute concentration and respective $\delta^{13}C$ and $\delta^{18}O$ values. $\delta$ values are expressed based on Vienna Pee Dee Belemnite (VPDB) $CO_2$ scale and were determined by high precision IRMS analysis.

### 2.2 Calibration set-up and protocol

We developed a two-step calibration procedure to (a) correct for concentration-dependent errors in isotopic data measurements and (b) correct for deviations in measured $\delta$ values from absolute values due to the offset (other than concentration-dependent error) introduced by the laser spectrometer. Also, we used Allan variance curves for determining the time interval to average the data (Nelson et al., 2008) in order to achieve the highest precision that can be offered by the LGR CCIA 36-d (Allan et al., 1997).

The first part of our calibration methodology was developed to correct for the concentration-dependent error observed in preliminary studies for $\delta^{13}C$ and $\delta^{18}O$ values measured using OA-ICOS. Such a calibration protocol was used in addition to the routine three-point calibration performed with in-house $CO_2$ gas standards of known $\delta^{13}C$ and $\delta^{18}O$ values. We developed a $CO_2$ dilution set-up (see Fig. 1) in which each of the three $CO_2$ standard gases was diluted with synthetic $CO_2$-free air (synthetic air) to different $CO_2$ concentrations. By applying a dilution series, we identified the deviation of the measured (OA-ICOS) from the absolute (IRMS) $\delta^{13}C$ and $\delta^{18}O$ values depending on $CO_2$ concentration (see Fig. 4). The $\delta^{13}C$ and $\delta^{18}O$ values of our in-house calibration gas standards were measured via cryoextraction and dual-inlet IRMS. $\delta^{13}C$ and $\delta^{18}O$ of the standard gases (see Table S1) across a wide range of $CO_2$ concentrations are measured using OA-ICOS. The deviation of the measured $\delta^{13}C$, and $\delta^{18}O$ from absolute values with respect to changing $CO_2$ concentrations was mathematically modelled and later used for data correction (see Fig. 5). A standard three-point calibration was then applied to correcting for concentration-dependent errors (see Fig. 7). The standards used covered a wide range of $\delta^{13}C$ and $\delta^{18}O$ values, including the values observed in the field of application.

Standard gases were released to a mass flow controller (ANALYT-MTC, series 358, MFC1) after passing through a pressure controller valve (see Fig. 1) with safety bypass (TESCOM, D43376-AR-00-X1-S, version 5). A Swagelok filter, (Stainless Steel All-Welded In-Line Filter; Swagelok, SS-4FWS-05, F1) was installed at the inlet of the flow controller (ANALYT-MTC, series 358, MFC1). Synthetic air was released and passed to another flow controller (ANALYT-MTC, series 358, MFC2) through a Swagelok filter (F2 in Fig. 1). $CO_2$ and synthetic air leaving the flow controllers (MFC1 and MFC2 respectively) were then mixed and drawn through a Teflon tube (P8) with a 6.35 mm outer diameter (OD), which was kept in a gas thermostat unit (see Fig. 1). The thermostat unit contained (a) a thermostat-controlled water bath (Kottermann, 3082) and (b) an Isotherm flask containing liquid nitrogen. The water bath was used to raise the temperature above room temperature and also to bring the temperature down to +5 °C by placing ice packs in the water bath. To reach low temperatures (−20 °C), we immersed the tubes in the isotherm flask filled with liquid $N_2$. Leaving the thermostat unit, the gas was directed to the multiport inlet unit of the OA-ICOS. By using the thermostat unit, we introduced a shift in the reference gas temperature, and the aim was to test the temperature sensitivity of the OA-ICOS in measuring $\delta^{13}C$ and $\delta^{18}O$ values. The third $CO_2$ standard gas (which is used for validation) was produced by mixing the other two gas standards in equal molar proportions in a 10 L volume plastic bag with an inner aluminum foil coating and welded seams

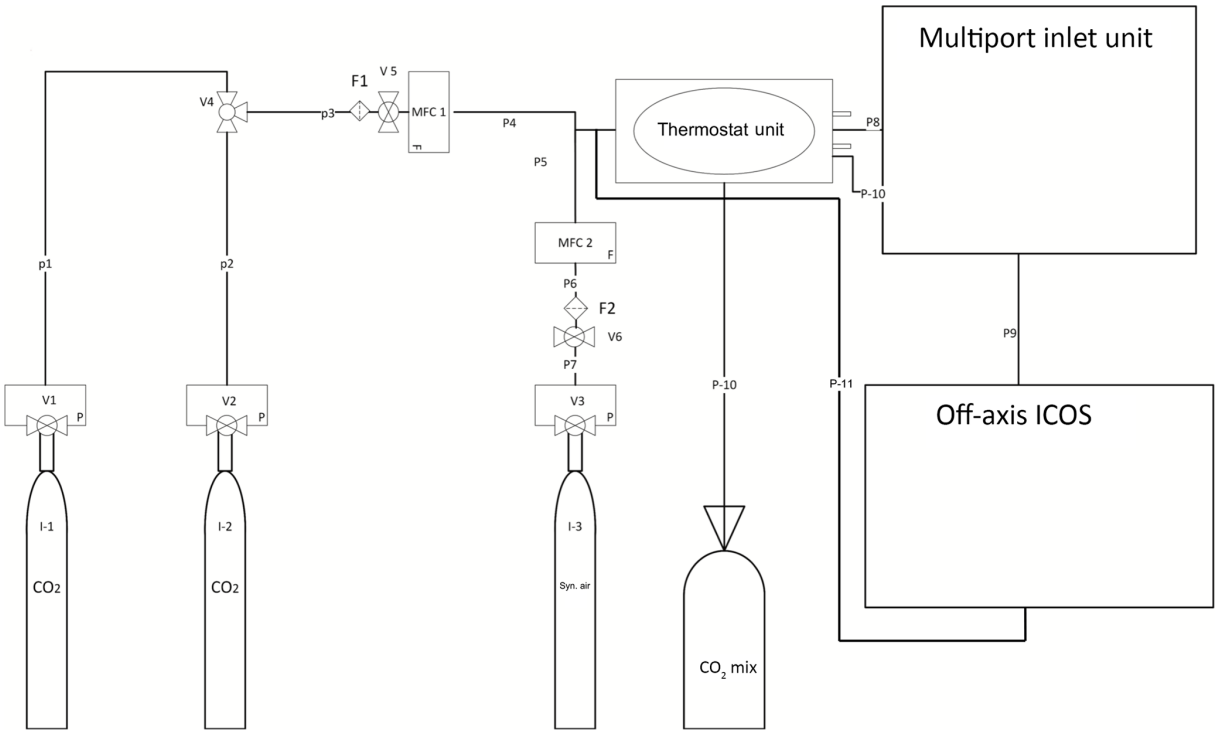


**Figure 1.** Set-up made for calibration of OA-ICOS (LGR CCIA 36-d). I (1, 2) represents $CO_2$ standards, $CO_2$ mix denotes gas standards mixed in equal molar proportion, I3 represents synthetic air, MFC (1, 2) denotes mass flow controller, F (1, 2) represents PTFE filter, V (1, 2, 3) denotes pressure-reducing valves, V4 shows three-way ball valve, V (5, 6) stands for pressure controller valve with safety bypass, P (1–7) denotes steel pipes, and P (8–11) represents Teflon tubing.

($CO_2$ mix: Linde PLASTIGAS®) under 0.03 MPa pressure by diluting to the required concentration using synthetic air. The mixture was then temperature adjusted and delivered to the MIU by using a 6.35 mm (OD) Teflon tube (P10). From the multiport inlet unit, calibration gases were delivered into the OA-ICOS for measurement using a 6.35 mm OD Teflon tube (P9) at a pressure $< 0.0689$ MPa, with a flow rate of 500 mL $min^{-1}$. The gas leaving the OA-ICOS through the exhaust was fed back to the 6.35 mm (OD) Teflon tube (P8) by using a Swagelok pipe tee (Stainless Steel Pipe Fitting, Male Tee, 6.35 mm OD, Male NPT), intersecting the P8 line before entering the thermostat unit. Thus, the gas fed was looped in the system until steady values were reported by the OA-ICOS based on $CO_2$ (ppm), $\delta^{13}C$, and $\delta^{18}O$ measurements. $CO_2$ gas standards were measured at 27 different $CO_2$ concentration levels ranging between 400 and 25 000 ppm. Every hour before sampling, synthetic air gas was flushed through the system to remove $CO_2$ to avoid memory effects. The calibration gases were measured in a sequence, one after the other, four times. During each round of measurement, every calibration gas was diluted to different concentrations of $CO_2$ (400–25 000 ppm), and the respective isotopic signature and concentration were determined. For each measurement of $\delta^{13}C$ and $\delta^{18}O$ at a given concentration, the first 50 readings were omitted to avoid possible memory effects of the laser spectrometer, and the subsequent readings for the next 256 s were taken and averaged to get maximum precision for $\delta^{13}C$ and $\delta^{18}O$ measurements. When switching between different calibration gases at the multiport inlet unit, synthetic air was purged through the systems for 30 s to avoid cross contamination.

### 2.3 Experimental sites

In situ experiments were conducted to measure $\delta^{13}C$, $\delta^{18}O$, and concentrations of soil $CO_2$ in two different soil types (calcareous and acidic soil). The measurements in a calcareous soil were conducted during June 2014 in cropland cultivated with wheat (*Triticum aestivum*) in Neuried, a small village in the upper Rhine Valley in Germany, situated at 48°26′55.5″ N, 7°47′20.7″ E, 150 m a.s.l. The soil type described as calcareous Fluvic Gleysol IUSS Working Group WRB (2015) developed on gravel deposits in the upper Rhine Valley. Soil depth was medium to deep, with high contents of coarse material ($> 2$ mm) up to 30 %–50 %. Mean soil organic carbon (SOC) content was 1.2 %–2 %, and SOC stock ranged between 50 and 90 t $ha^{-1}$. The average pH was found to be 8.6. The study site receives an annual rainfall of 810 mm and has a mean annual temperature of 12.1 °C.

In situ measurements in an acidic soil were conducted by the end of July 2014 in the model ecosystem facility (MODOEK) of the Swiss Federal Research Institute WSL in Birmensdorf, Switzerland (47°21′48″ N, 8°27′23″ E; 545 m a.s.l.). The MODOEK facility comprises 16 model ecosystems, split below ground into two lysimeters with an area of 3 $m^2$ and a depth of 150 cm. The lysimeters used for the present study were filled with acidic (Haplic Alisol) forest soil IUSS (2014) and planted with young beech trees (Arend et al., 2016). The soil pH was 4.0, with a total SOC content of 0.8 % (Kuster et al., 2013).

### 2.4 Experimental set-up

The OA-ICOS was connected to gas-permeable, hydrophobic membrane tubes (Accurel® tubing, 8 mm outer diameter) of 2 m length, placed horizontally in the soil at different depths. Tubes were laid in six different depths (4, 8, 12, 17, 35, and 80 cm) for calcareous soil and three depths (10, 30, and 60 cm) for acidic soil.

Technical details of the measurement set-up are shown in Fig. 2. Both ends of the membrane tubes were extended vertically upwards, reaching the soil top by connecting them to gas impermeable Synflex® tubing (8 mm OD) using Swagelok tube fitting union (Swagelok: SS-8M0-6, 8 mm tube OD). One end of the tubing system was connected to a solenoid switching valve (Bibus: MX-758.8E3C3KK), by using a stainless-steel reducing union (Swagelok: SS-8M0-6-6M), to the outlet of the LGR CCIA 36-d by using 6.35 mm (OD) Teflon tubing. The other end was connected via the multiport inlet unit to the gas inlet of the LGR CCIA 36-d.

This way, a loop was created in which the soil $CO_2$ drawn into the OA-ICOS was circulated back through the tubes and in and out of the OA-ICOS and measured until a steady state was reached. We experienced no drop in cavity pressure while maintaining a closed loop (see Fig. S2). Each depth was selected and continuously measured for 6 min at specified time intervals by switching to defined depths at the multiport inlet unit and also at the solenoid valve.

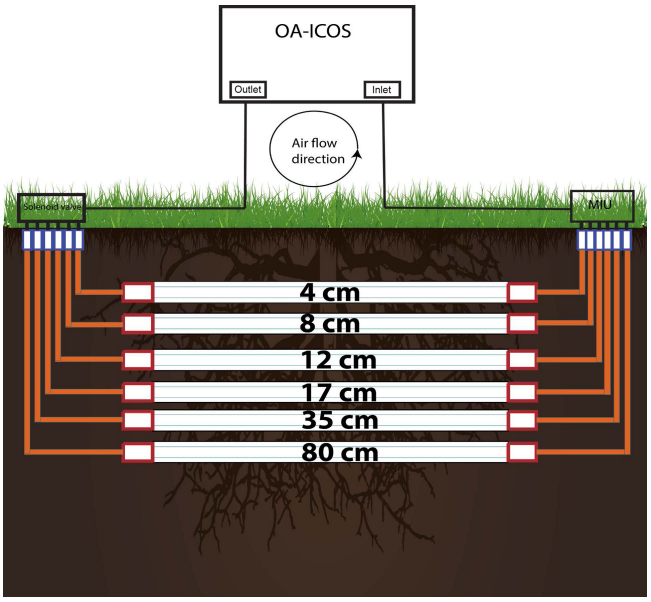


**Figure 2.** Installation made for soil air $CO_2$ (ppm), $\delta^{13}$C-$CO_2$ and $\delta^{18}O-CO_2$ measurements using off-axis integrated cavity output spectrometer (OA-ICOS). Hydrophobic membrane tubing was installed horizontally in soil at different depths. MIU: multiport inlet unit.

## 3 Results and discussion

### 3.1 Instrument calibration and correction

The highest level of precision obtained for $\delta^{13}$C and $\delta^{18}$O measurements at the maximum measuring frequency (1 Hz) was determined by using Allan deviation curves (see Fig. 3). The maximum precision of 0.022 ‰ for $\delta^{13}$C was obtained when the data were averaged over 256 s, and the maximum for $\delta^{18}$O, 0.077 ‰, was obtained for the same averaging interval as for $\delta^{13}$C.

To correct for $CO_2$ concentration-dependent errors in raw $\delta^{13}$C and $\delta^{18}$O data, we analysed data obtained from the OA-ICOS to determine the sensitivity of $\delta^{13}$C and $\delta^{18}$O measurements against changing concentrations of $CO_2$. We observed a specific pattern of deviance in the measured isotopic data from the absolute values (both for $\delta^{13}$C and $\delta^{18}$O) across $CO_2$ concentration ranging from 25 000 to 400 ppm (see Fig. 4). Uncalibrated $\delta^{13}$C and $\delta^{18}$O measurements showed a standard deviation of 6.44 ‰ and 6.80 ‰ respectively, when measured under changing $CO_2$ concentrations.

The dependency of $\delta^{13}$C and $\delta^{18}$O values on the $CO_2$ concentration was compensated by using a non-linear model. The deviations (Diff-$\delta$) of the measured delta values ($\delta_{(\text{OA-ICOS})}$) from the absolute value of the standard gas ($\delta_{(\text{IRMS})}$) at different concentrations of $CO_2$ were calculated (Diff-$\delta = \delta_{(\text{OA-ICOS})} - \delta_{(\text{IRMS})}$). Several mathematical models were then fitted to Diff-$\delta$ as a function of changing $CO_2$ concentration (see Fig. 5). The mathematical model with the best fit for Diff-$\delta$ data was selected using the corrected Akaike information criterion ($AIC_C$; Glatting et al., 2007; Hurvich and Tsai, 1989; Yamaoka et al., 1978). The non-linear model fits applied for Diff-$\delta^{13}$C and Diff-$\delta^{18}$O measurements are given in Tables 1 and 2, respectively. For Diff-$\delta^{13}$C, a three-parameter exponential model fitted best with $r^2 = 0.99$ (see Table 3 for the values of the parameters; see Fig. S3a for model residuals), and a three-parameter power function model (see Table 2) with $r^2 = 0.99$ showed the best fit for Diff-$\delta^{18}$O (see Table 3 for the values of the parameters; see Fig. S3b for model residuals). The best fit was then introduced into the measured isotopic data ($\delta^{13}$C and $\delta^{18}$O) and corrected for concentration-dependent errors (see Fig. 6). After correction, the standard deviation of $\delta^{13}$C was reduced

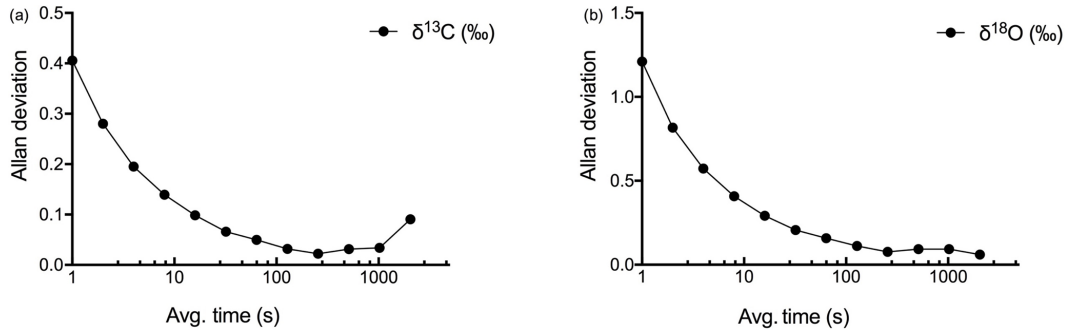


**Figure 3.** Allan deviation curve for $\delta^{13}C$ **(a)** and $\delta^{18}O$ **(b)** measurements by OA-ICOS $CO_2$ carbon isotope analyser (LGR CCIA-36d).

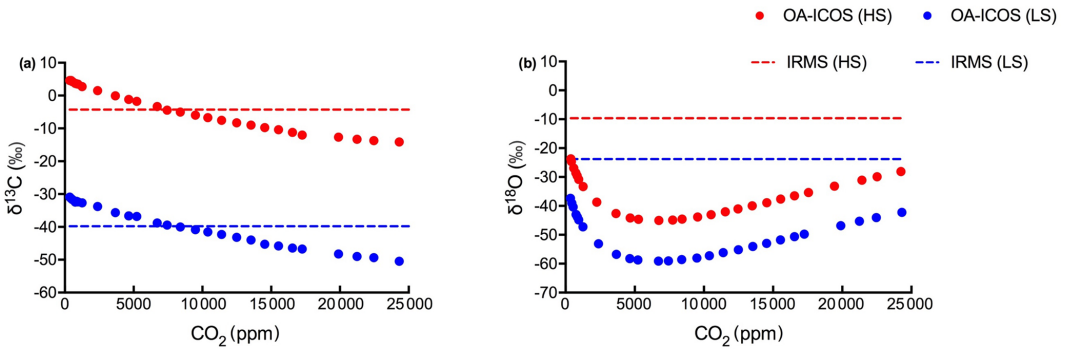


**Figure 4.** Variability observed in **(a)** $\delta^{13}C$ and **(b)** $\delta^{18}O$ measurements using OA-ICOS before calibration. $\delta^{13}C$ and $\delta^{18}O$ measured using OA-ICOS for heavy standard and light standard are shown as red and blue circles respectively. Actual $\delta^{13}C$ and $\delta^{18}O$ values reported after measuring by IRMS for heavy standard and light standard are shown as red and blue dashed lines respectively.

to 0.08 ‰, and the deviation of $\delta^{18}O$ to 0.09 ‰, for all measurements across the whole $CO_2$ concentration range.

After correcting the measured $\delta^{13}C$ and $\delta^{18}O$ values for the $CO_2$ concentration-dependent deviations, a three-point calibration (Sturm et al., 2012) was made by generating linear regressions with the concentration-corrected $\delta^{13}C$ and $\delta^{18}O$ values against absolute $\delta^{13}C$ and $\delta^{18}O$ values (see Fig. 7; see Fig. S4 for linear regression residuals). Using the linear regression lines, we were able to measure the validation gas standard, with standard deviations of 0.0826 ‰ for $\delta^{13}C$ and 0.0941 ‰ for $\delta^{18}O$.

For the LGR CCIA 36-d, we found that routine calibration (correction for concentration-dependent error plus three-point calibration) was necessary for obtaining the required accuracy, in particular under fluctuating $CO_2$ concentrations. The LGR CCIA-36d offers an option for calibration against a single standard, a feature which was already in place in a predecessor model (CCIA DLT-100; Guillon et al., 2012). This internal calibration is sufficient when LGR CCIA-36d is operated only under stable $CO_2$ concentrations. To correct for the concentration dependency, we introduced mathematical model fits, which corrected for the deviation pattern found for both $\delta^{13}C$ and $\delta^{18}O$. We assume that these deviations are instrument specific and that the fitting parameters need to be adjusted for every single device. Experiments conducted to investigate the influence of external temperature fluctuations on OA-ICOS measurements did not show any significant changes in the temperature inside the optical cavity of the OA-ICOS (see Fig. S1). The previous version of the Los Gatos CCIA was strongly influenced by temperature fluctuations during sampling (Guillon et al., 2012). The lack of temperature dependency as observed here with the most recent model can be mostly due to the heavy insulation provided with the system, which was not found in the older models.

Guillon et al. (2012) found a linear correlation between $CO_2$ concentration and respective stable isotope signatures with a previous version of the Los Gatos CCIA $CO_2$ stable isotope analyser. In our experiments with the OA-ICOS, the best fitting correlations between $CO_2$ concentration and $\delta^{13}C$ and $\delta^{18}O$ measurements were exponential and power functions, respectively. We assume that measurement accuracy is influenced by the number of $CO_2$ molecules present inside the laser cavity of the particular laser spectrometer, as we observed large standard deviation in isotopic measurements at lower $CO_2$ concentrations. This behaviour of an OA-ICOS can be expected, as it functions by sweeping the laser along an absorption spectrum, measuring the energy transmitted after passing through the sample. Therefore, energy transmitted is proportional to the gas concentration in the cavity. The laser absorbance is then determined by normalising against a

**Table 1.** Correction factor models are fitted for Diff-$\delta^{13}$C, DF (degrees of freedom), $AIC_C$ (Akaike information criterion), and [$CO_2$] $CO_2$ concentration in ppm.

| Model fit | Equation | $R^2$ | $AIC_C$ | DF |
|---|---|---|---|---|
| Exponential | Diff-$\delta^{13}C = a \times (b - \exp(-c \times [CO_2]))$ | 0.99 | −294.6 | 54 |
| Polynomial | Diff-$\delta^{13}C = a + (b \times [CO_2]) + (c/[CO_2]^2)$ | 0.98 | −27.56 | 54 |
| Logarithmic | Diff-$\delta^{13}C = a + b \times \ln([CO_2])$ | 0.89 | 91.68 | 55 |
| LOWESS | – | 0.99 | −170.24 | 54 |

**Table 2.** Correction factor models are fitted for Diff-$\delta^{18}$O, DF (degrees of freedom), $AIC_C$ (Akaike information criterion), and [$CO_2$] $CO_2$ concentration in ppm.

| Model fit | Equation | $R^2$ | $AIC_C$ | DF |
|---|---|---|---|---|
| Power | Diff-$\delta^{18}O = a \times (b^{[CO_2]}) \times ([CO_2]^c)$ | 0.99 | −337.04 | 51 |
| Polynomial | Diff-$\delta^{18}O = (a + b \times x)/(1 + c \times [CO_2] + d \times [CO_2]^2)$ | 0.98 | −19.34 | 50 |
| Steinhart–Hart | Diff-$\delta^{18}O = 1/a + (b \times \ln[CO_2]) + (c \times (\ln[CO_2])^3)$ | 0.96 | 29.77 | 51 |
| LOWESS | – | 0.78 | 128.66 | 51 |

**Table 3.** Parameter values for correction factor model fit for Diff-$\delta^{13}$C and Diff-$\delta^{18}$O.

| Parameter | Value | SE | 95 % confidence |
|---|---|---|---|
| $a^{13}$C | 31.007 | 0.2149 | 30.57–31.43 |
| $b^{13}$C | 0.713 | 0.002376 | 0.708995–0.718522 |
| $c^{13}$C | 0.000043 | 0.000000 | 0.000042–0.000043 |
| $a^{18}$O | 0.85 | 0.003 | 0.8455–0.8576 |
| $b^{18}$O | 0.99 | 0.00 | 0.999928–0.9999283 |
| $c^{18}$O | 0.477 | 0.0047 | 0.476871–0.478767 |

reference signal, finally calculating the concentration of the sample measured by integrating the whole spectrum of absorbance (O'Keefe et al., 1999).

### 3.2 Variation in soil $CO_2$ concentration, carbon, and oxygen isotope values

Figures 9 and 10 show the $CO_2$ concentration and the $\delta^{13}$C and $\delta^{18}$O measurements of soil $CO_2$ in the calcareous as well as in the acidic soil across the soil profile with a sub-daily resolution and as averages for the day, respectively. We observed an increase in the $CO_2$ concentration across the soil depth profile for both the calcareous and the acidic soil. Moreover, there were rather contrasting $\delta^{13}$C values across the profile for the two soil types. In the calcareous soil, $CO_2$ was relatively enriched in $^{13}$C in the surface soil (4 cm) as compared to the 8 cm depth. Below 8 cm down to 80 cm depth, we found an increase in $\delta^{13}$C values. At 80 cm depth, the $\delta^{13}$C in soil $CO_2$ ranged between −7.15 ‰ and −3.35 ‰ (see Fig. 9), with a daily average of −6.19±1.45 ‰ (see Fig. 10), hence being clearly above atmospheric values (≈ −8.0 ‰). For $\delta^{18}$O values of calcareous soil, the depth profile showed no specific pattern, except for the $\delta^{18}$O values at 80 cm depth, which were found to be less negative than the values at the other depths. The $\delta^{18}$O value in the top 4 cm was found to be slightly more enriched that the 8 cm depth, and between 8–35 cm, $\delta^{18}$O values showed little variation relative to each other. For the sub-daily measurements, we observed a sharp decline in $\delta^{18}$O values at around 02:00 CET, which is also observed but less pronounced for the $\delta^{13}$C signal. We assume that the reason for such aberrant values is a technical issue rather than a biological process. It could be due to the fact that the internal pump in the OA-ICOS was not taking an adequate amount of gas into the optical cavity, thereby creating a negative pressure inside the cavity resulting in the observed aberrant values. The patterns observed for the $\delta^{13}$C values of $CO_2$ in the calcareous soil with $^{13}$C enrichment in deeper soil layers can be explained by a substantial contribution of $CO_2$ from abiotic origin to total soil $CO_2$ release as a result of carbonate weathering and subsequent outgassing from soil water (Schindlbacher et al., 2015). According to Cerling (1984), the distinct oxygen and carbon isotopic composition of soil carbonate depends primarily on the isotopic signature of meteoric water and on the proportion of $C_4$ biomass present at the time of carbonate formation (Cerling, 1984) but also on numerous other factors that determine the $^{13}$C value of soil $CO_2$. $CO_2$ released as a result from carbonates in calcareous soil site have a distinct $\delta^{13}$C value of −9.3 (mean value across soil profile 0–80 cm depth; Fig. 8c), while $CO_2$ released during biological respiratory processes has $\delta^{13}$C values around −24 ‰, as observed in the acidic soil (Fig. 10e). The $\delta^{13}$C values of soil

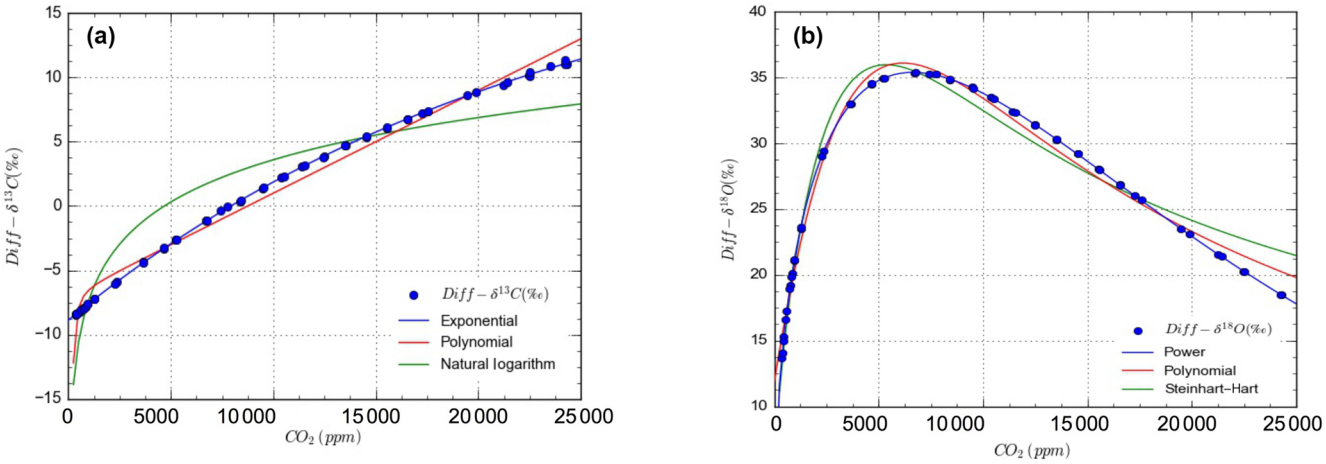


**Figure 5.** Mathematical models for concentration dependent drift in OA-ICOS measurements of stable isotopes of carbon **(a)** and oxygen **(b)** in $CO_2$ from IRMS measurements. Blue circles show Diff-$\delta^{13}$C **(a)** and Diff-$\delta^{18}$O **(b)** data points, and lines represent different mathematical models fitted on the measured data.

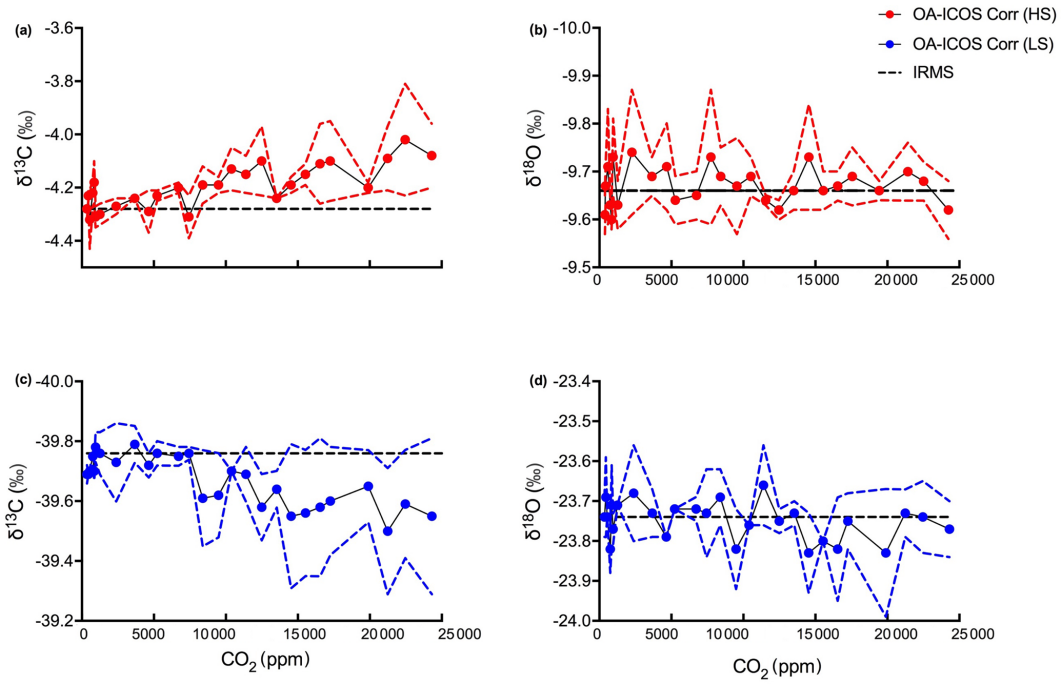


**Figure 6.** Corrected **(a, c)** $\delta^{13}$C and **(b, d)** $\delta^{18}$O measurements by OA-ICOS $CO_2$ carbon isotope analyser. $\delta^{13}$C and $\delta^{18}$O measured for heavy standard and light standard are shown as red and blue circles respectively. Actual $\delta^{13}$C and $\delta^{18}$O values reported after measuring by IRMS are shown as black dashed lines, and 95 % confidence intervals are shown as coloured dashed lines, respectively.

$CO_2$ observed in the deepest soil layer in the calcareous soil site most likely indicate the presence of carbonate sources of a pedogenic and geologic origin. Even though the contribution of $CO_2$ from abiotic sources to soil $CO_2$ is often considered to be low, several studies have reported significant proportions ranging between (10 %–60 %), emanating from abiotic sources (Emmerich, 2003; Plestenjak et al., 2012; Ramnarine et al., 2012; Serrano-Ortiz et al., 2010; Stevenson and Verburg, 2006; Tamir et al., 2011). Bowen and Beerling (2004) showed that isotope effects associated with soil organic matter (SOM) decomposition can cause a strong gradient in $\delta$ values of soil organic matter with depth but are not always reflected in the $\delta^{13}$C values of soil $CO_2$. We have measured soil samples for bulk soil $\delta^{13}$C, carbonate $\delta^{13}$C, and $\delta^{18}$O values and have also determined the percentage of total carbon in the soil across a depth profile of (0–80 cm; see

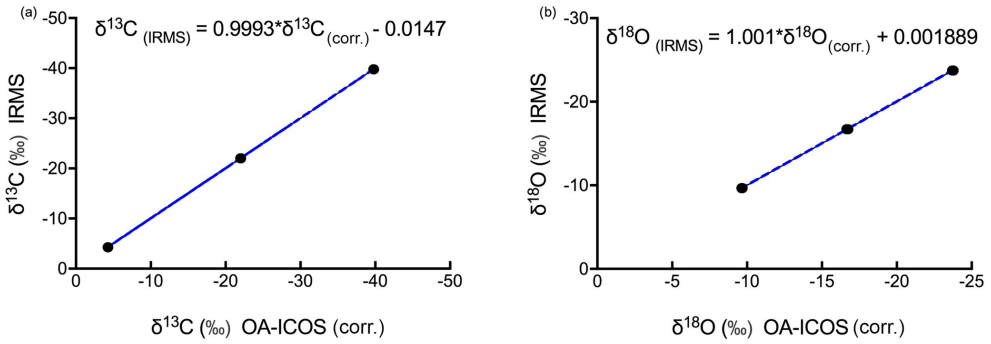


**Figure 7.** Three-point calibration lines for **(a)** $\delta^{13}$C and **(b)** $\delta^{18}$O measurements using OA-ICOS with 95 % confidence interval.

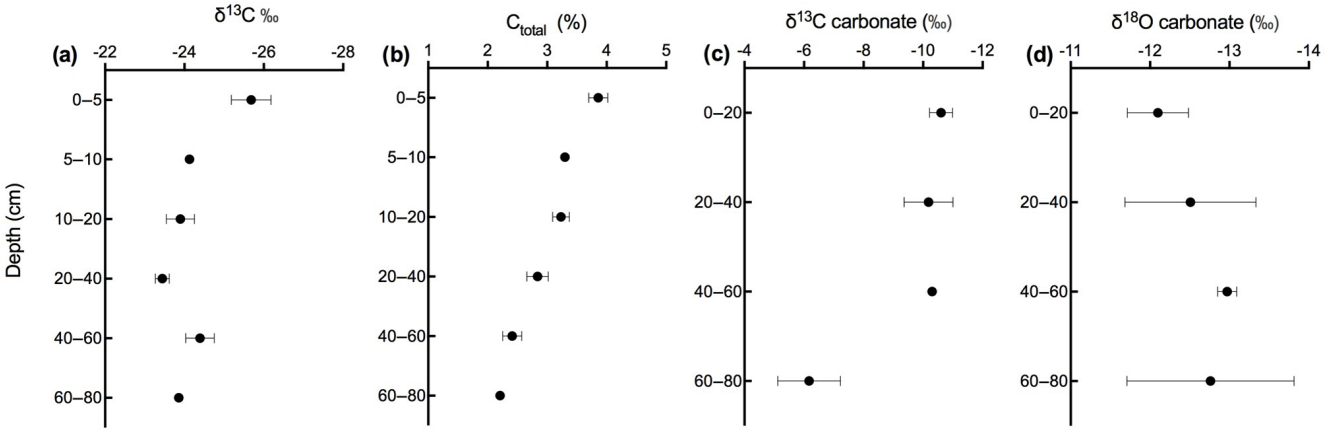


**Figure 8.** Depth profile of **(a)** $\delta^{13}$C, **(b)** carbon content, **(c)** $\delta^{13}$C of soil carbonate, and **(d)** $\delta^{18}$O of soil carbonate in calcareous soil.

Fig. 8). We observed an increase in $\delta^{13}$C values for bulk soil in deeper soil layers (see Fig. 8a, c). Moreover, the carbonate $\delta^{13}$C values also got more positive in the 60–80 cm layer. Since total organic carbon content decreases with depth, it can be assumed that the $CO_2$ derived from carbonate weathering, having less negative $\delta^{13}$C values, more strongly contributed to the soil $CO_2$ (especially since we see an increase in soil $CO_2$ concentration with depth). This is accordance with the laser-based measurements which showed a strong increase in the $\delta^{13}$C of soil $CO_2$ in the deepest soil layer, leading us to the hypothesis that this signal indicates a strong contribution of carbonate-derived $CO_2$. Water content, soil $CO_2$ concentration, and the presence of organic acids or any other source of $H^+$ are the major factors influencing carbonate weathering, and variations in soil $CO_2$ partial pressure, moisture, temperature, and pH can cause degassing of $CO_2$ which contributes to the soil $CO_2$ efflux (Schindlbacher et al., 2015; Zamanian et al., 2016). $CaCO_3$ solubility in pure $H_2O$ at 25 °C is 0.013 g $L^{-1}$, but in weak acids like carbonic acid, the solubility is increased up to 5 fold (Zamanian et al., 2016). The production of carbonic acid due to $CO_2$ dissolution will convert carbonate to bicarbonates, resulting in exchange of carbon atoms between carbonates and dissolved $CO_2$.We assume that at our study site, the topsoil is decarbonated due to intensive agriculture for a longer period, thus the soil $CO_2$ there originates primarily from autotrophic and heterotrophic respiratory activity. In contrast to the deeper soil layers, where the carbonate content is high, $CO_2$ from carbonate weathering is assumed to be a dominating source of soil $CO_2$. Also, outgassing of $CO_2$ from the large groundwater body underneath the calcareous Gleysol might contribute to the inorganic $CO_2$ sources in the deeper soil, as we found the groundwater table to be 1–2 m below the soil surface. Relative $^{13}$C enrichment of the $CO_2$ in the topsoil (4 cm) compared to that at 8 cm depth is probably due to the invasive diffusion of atmospheric $CO_2$, which has a $\delta^{13}$C value close to −8 ‰ (e.g. Levin et al., 1995). The $\delta^{18}$O patterns for $CO_2$ between 4 and 35 cm might reflect the $\delta^{18}$O of soil water with stronger evaporative enrichment at the top and $^{18}$O depletion towards deeper soil layers. In comparison, the strong $^{18}$O enrichment of soil $CO_2$ towards 80 cm in the calcareous Gleysol very likely reflects the $^{18}$O values of groundwater lending further support to the high contribution of $CO_2$ originating from the outgassing of groundwater. We, however, need then to assume that the oxygen in the $CO_2$ is not in full equilibrium with the precipitation-influenced soil water. Since mainly microbial carbonic anhydrase mediates the fast equilibrium between $CO_2$, and water in the soil and

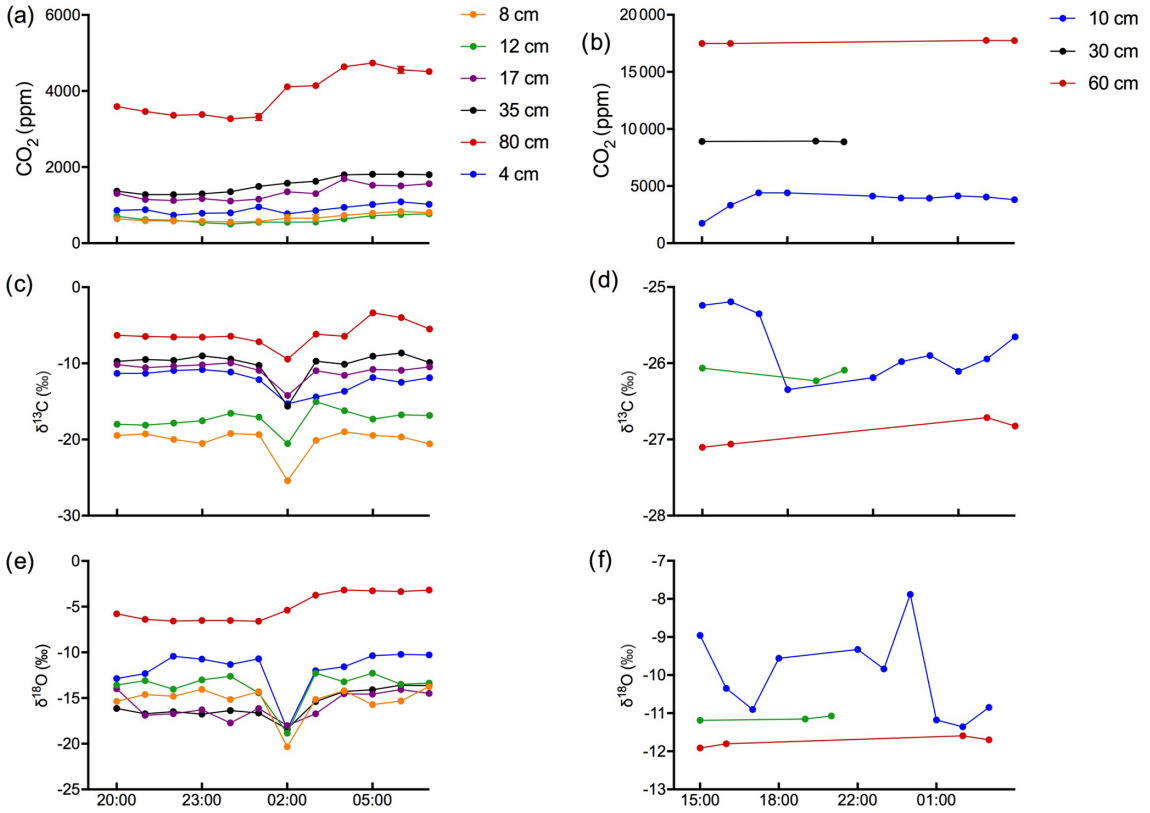


**Figure 9.** Time course of the evolution of soil gas $CO_2$ (ppm), $\delta^{13}C$, and $\delta^{18}O$ in calcareous **(a, c, e)** and acidic **(b, d, f)** soils. Data collected continuously over a 12 h time frame for the calcareous soil and a 14 h time window with intermittent data collection for the acidic soil.

the microbial activity is low in deeper soil layers (Schmidt et al., 2011), we speculate that in deep layers with a significant contribution of groundwater derived $CO_2$ to the $CO_2$ pool, a lack of full equilibration with soil water might be the reason for the observed $\delta^{18}O$ values.

Soil $CO_2$ concentration in the acidic soil showed a positive relationship with soil depth as $CO_2$ concentration increased along with increasing soil depth (Figs. 9 and 10). $CO_2$ concentrations were distinctly higher than in the calcareous soil, very likely due to the finer texture than in the gravel-rich calcareous soil. $\delta^{13}C$ values amounted to approximately $-26‰$ in 30 and 60 cm depth, indicating the biotic origin from (autotrophic and heterotrophic) soil respiration (Schönwitz et al., 1986). In the topsoil, $\delta^{13}C$ values did not strongly increase, pointing towards a less pronounced inward diffusion of $CO_2$ in the acidic soil site, most likely due to more extensive outward diffusion of soil $CO_2$, as indicated by the still very high $CO_2$ concentration at 10 cm creating a sharp gradient between soil and atmosphere. Moreover, the acidic soil was rather dense and contained no stones, strongly suggesting that gas diffusivity was rather small. $\delta^{18}O$ depth patterns of soil $CO_2$ in the acidic soil most likely reflected $\delta^{18}O$ values of soil water as $CO_2$ became increasingly $^{18}O$ depleted from top to bottom. The $\delta^{18}O$ of deeper soil layers $CO_2$ (30–60 cm) was close to the values expected when full oxygen exchange between soil water and $CO_2$ occurred (Kato et al., 2004). Assuming an $^{18}O$ fractionation of 41‰ between $CO_2$ and water (Brenninkmeijer et al., 1983), this would result in an expected value for $CO_2$ of $\approx -10 \pm 2‰$ vs. VPDB $CO_2$. Corresponding results have been shown for $\delta^{18}O$ of soil $CO_2$ using similar hydrophobic gas-permeable membrane tubes used when measuring $\delta^{18}O$ of soil $CO_2$ and soil water in situ (Gangi et al., 2015).

## 4 Conclusions

During our preliminary tests with the OA-ICOS, we found that the equipment was highly sensitive to changes in $CO_2$ concentrations. We found a non-linear response of the $\delta^{13}C$ and $\delta^{18}O$ values against changes in $CO_2$ concentration. Given the fact that laser-based $CO_2$ isotope analysers are deployed on site in combination with different gas sampling methods like automated chambers systems (Bowling et al., 2015) and hydrophobic gas-permeable membranes (Jochheim et al., 2018) for tracing various ecosystem processes, it is important to address this issue. Therefore, we developed a calibration strategy for correcting errors introduced in $\delta^{13}C$ and $\delta^{18}O$ measurements due to the sensitivity of the device against changing $CO_2$ concentrations. We

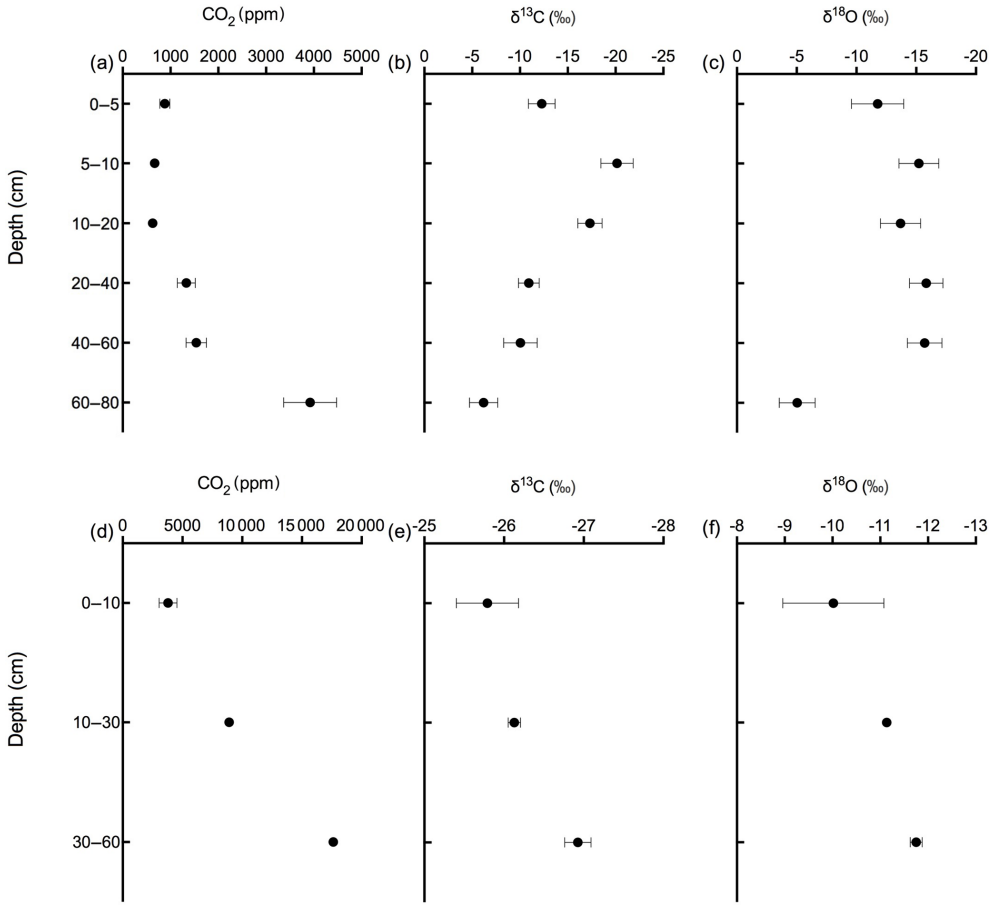


**Figure 10.** Daily average data of soil $CO_2$ (ppm), $\delta^{13}C$, and $\delta^{18}O$ in calcareous **(a, b, c)** and acidic **(d, e, f)** soils across soil depth profiles.

found that the OA-ICOS measures stable isotopes of $CO_2$ gas samples with a precision comparable to conventional IRMS. The method described in this work for measuring $CO_2$ concentration and $\delta^{13}C$ and $\delta^{18}O$ values in soil air profiles using an OA-ICOS and hydrophobic gas-permeable tubes is promising and can be applied for soil $CO_2$ flux studies. As this set-up is capable of measuring continuously for longer time periods at a higher temporal resolution (0.05–0.1 Hz), it offers greater potential to investigate the isotopic identity of $CO_2$ and the interrelation between soil $CO_2$ and soil water. By using our measurement set-up, we could identify abiotic as well as biotic contributions to the soil $CO_2$ in the calcareous soil. We infer that degassing of $CO_2$ from carbonates due to weathering and evasion of $CO_2$ from groundwater may leave the soil $CO_2$ with a specific and distinct $\delta^{13}C$ signature, especially when the biotic activity is rather low.

**Data availability.** Data are available via https://doi.org/10.5281/zenodo.2551237 (Joseph, 2019).

**Supplement.** The supplement related to this article is available online at: https://doi.org/10.5194/soil-5-49-2019-supplement.

**Author contributions.** CK, MW, AG, and JJ conceived the idea. JJ conducted the experiments, analyzed the data, and created the figures. JJ, AG, and MW wrote the paper. MS, FH, MA, and CK commented on and edited the paper.

**Competing interests.** The authors declare that they have no conflict of interest.

**Acknowledgements.** We thank the Federal Ministry of Education and Research, Germany (BMBF), and the KIT (Karlsruhe Institute of Technology) for providing financial support for the project ENABLE WCM (Grant Number: 02WQ1205). Arthur Gessler and Jobin Joseph acknowledge financial support by the Swiss National Science Foundation (SNF; 31003A_159866). We thank Barbara Herbstritt, Hannes Leistert, Emil Blattmann and Jens Lange, Matthias Saurer, Alessandro Schlumpf, Lukas Bächli, and Christian Poll for outstanding support in making this project into a reality.

Edited by: Raúl Zornoza
Reviewed by: Rolf Siegwolf and two anonymous referees

## References

Allan, D. W., Ashby, N., and Hodge, C. C.: The Science of Timekeeping, Hewlett-Packard, 88, available at: http://www.allanstime.com/Publications/DWA/Science_Timekeeping/TheScienceOfTimekeeping.pdf (last access: 16 March 2018), 1997.

Arend, M., Gessler, A., and Schaub, M.: The influence of the soil on spring and autumn phenology in European beech, Tree Physiol., 36, 78–85, https://doi.org/10.1093/treephys/tpv087, 2016.

Baer, D. S., Paul, J. B., Gupta, M., and O'Keefe, A.: Sensitive absorption measurements in the near-infrared region using off-axis integrated-cavity-output spectroscopy, Appl. Phys. B-Lasers O., 75, 261–265, https://doi.org/10.1007/s00340-002-0971-z, 2002.

Barthel, M., Sturm, P., Hammerle, A., Buchmann, N., Gentsch, L., Siegwolf, R., and Knohl, A.: Soil $H_2^{18}O$ labelling reveals the effect of drought on $C^{18}OO$ fluxes to the atmosphere, J. Exp. Bot., 65, 5783–5793, https://doi.org/10.1093/jxb/eru312, 2014.

Bertolini, T., Inglima, I., Rubino, M., Marzaioli, F., Lubritto, C., Subke, J.-A., Peressotti, A., and Cotrufo, M. F.: Sampling soil-derived $CO_2$ for analysis of isotopic composition: a comparison of different techniques, Isot. Environ. Healt. S., 42, 57–65, https://doi.org/10.1080/10256010500503312, 2006.

Bond-Lamberty, B. and Thomson, A.: Temperature-associated increases in the global soil respiration record, Nature, 464, 579–582, https://doi.org/10.1038/nature08930, 2010.

Bowen, G. J. and Beerling, D. J.: An integrated model for soil organic carbon and $CO_2$: Implications for paleosol carbonate $pCO_2$ paleobarometry, Global Biogeochem. Cy., 18, GB1026, https://doi.org/10.1029/2003GB002117, 2004.

Bowling, D. R., Sargent, S. D., Tanner, B. D., and Ehleringer, J. R.: Tunable diode laser absorption spectroscopy for stable isotope studies of ecosystem–atmosphere $CO_2$ exchange, Agr. Forest. Meteorol., 118, 1–19, https://doi.org/10.1016/S0168-1923(03)00074-1, 2003.

Bowling, D. R., Egan, J. E., Hall, S. J., and Risk, D. A.: Environmental forcing does not induce diel or synoptic variation in the carbon isotope content of forest soil respiration, Biogeosciences, 12, 5143–5160, https://doi.org/10.5194/bg-12-5143-2015, 2015.

Breecker, D. and Sharp, Z. D.: A field and laboratory method for monitoring the concentration and isotopic composition of soil $CO_2$, Rapid Commun. Mass Sp., 22, 449–454, https://doi.org/10.1002/rcm.3382, 2008.

Brenninkmeijer, C. A. M., Kraft, P., and Mook, W. G.: Oxygen isotope fractionation between $CO_2$ and $H_2O$, Chem. Geol., 41, 181–190, https://doi.org/10.1016/S0009-2541(83)80015-1, 1983.

Cerling, T. E.: The stable isotopic composition of modern soil carbonate and its relationship to climate, Earth Planet. Sc. Lett., 71, 229–240, https://doi.org/10.1016/0012-821X(84)90089-X, 1984.

Emmerich, W. E.: Carbon dioxide fluxes in a semiarid environment with high carbonate soils, Agr. Forest. Meteorol., 116, 91–102, 2003.

Francey, R. J. and Tans, P. P.: Latitudinal variation in oxygen-18 of atmospheric $CO_2$, Nature, 327, 495–497, https://doi.org/10.1038/327495a0, 1987.

Gangi, L., Rothfuss, Y., Ogée, J., Wingate, L., Vereecken, H., and Brüggemann, N.: A New Method for In Situ Measurements of Oxygen Isotopologues of Soil Water and Carbon Dioxide with High Time Resolution, Vadose Zone J., 14, 0, https://doi.org/10.2136/vzj2014.11.0169, 2015.

Glatting, G., Kletting, P., Reske, S. N., Hohl, K., and Ring, C.: Choosing the optimal fit function: Comparison of the Akaike information criterion and the F-test, Med. Phys., 34, 4285–4292, https://doi.org/10.1118/1.2794176, 2007.

Guillon, S., Pili, E., and Agrinier, P.: Using a laser-based $CO_2$ carbon isotope analyser to investigate gas transfer in geological media, Appl. Phys. B, 107, 449–457, https://doi.org/10.1007/s00340-012-4942-8, 2012.

Gut, A., Blatter, A., Fahrni, M., Lehmann, B. E., Neftel, A., and Staffelbach, T.: A new membrane tube technique (METT) for continuous gas measurements in soils, Plant Soil, 198, 79–88, https://doi.org/10.1023/A:1004277519234, 1998.

Harwood, K. G., Gillon, J. S., Roberts, A., and Griffiths, H.: Determinants of isotopic coupling of $CO_2$ and water vapour within a Quercus petraea forest canopy, Oecologia, 119, 109–119, https://doi.org/10.1007/s004420050766, 1999.

Hurvich, C. M. and Tsai, C.: Regression and time series model selection in small samples, Biometrika, 76, 297–307, https://doi.org/10.1093/biomet/76.2.297, 1989.

IUSS (International Union of Soil Sciences) Working Group WRB: World Reference Base for Soil Resources 2014, update 2015 International soil classification system for naming soils and creating legends for soil maps, World Soil Resources Reports No. 106, FAO, Rome, Italy, 2015.

Jochheim, H., Wirth, S., and von Unold, G.: A multi-layer, closed-loop system for continuous measurement of soil $CO_2$ concentration, J. Plant Nutr. Soil Sci., 181, 61–68, https://doi.org/10.1002/jpln.201700259, 2018.

Joseph, J.: Application of a laser-based spectrometer for continuous insitu measurements of stable isotopes of soil $CO_2$ in calcareous and acidic soils (Data set), Zenodo, https://doi.org/10.5281/zenodo.2551238, 2019.

Jost, H.-J., Castrillo, A., and Wilson, H. W.: Simultaneous $^{13}C/^{12}C$ and $^{18}O/^{16}O$ isotope ratio measurements on $CO_2$ based on off-axis integrated cavity output spectroscopy, Isot. Environ. Healt. S., 42, 37–45, https://doi.org/10.1080/10256010500503163, 2006.

Kammer, A., Tuzson, B., Emmenegger, L., Knohl, A., Mohn, J., and Hagedorn, F.: Application of a quantum cascade laser-based spectrometer in a closed chamber system for real-time $\delta^{13}C$ and $\delta^{18}O$ measurements of soil-respired $CO_2$, Agr. Forest. Meteorol., 151, 39–48, https://doi.org/10.1016/j.agrformet.2010.09.001, 2011.

Kato, T., Nakazawa, T., Aoki, S., Sugawara, S., and Ishizawa, M.: Seasonal variation of the oxygen isotopic ratio of atmospheric carbon dioxide in a temperate forest, Japan, Global Biogeochem. Cy., 18, GB2020, https://doi.org/10.1029/2003GB002173, 2004.

Kayler, Z. E., Sulzman, E. W., Rugh, W. D., Mix, A. C., and Bond, B. J.: Soil biology and biochemistry, Pergamon, available at: https://www.cabdirect.org/cabdirect/abstract/20103097455 (last access: 16 March 2018), 2010.

Keeling, C. D.: The concentration and isotopic abundances of atmospheric carbon dioxide in rural areas, Geochim. Cosmochim. Ac., 13, 322–334, https://doi.org/10.1016/0016-7037(58)90033-4, 1958.

Kerstel, E. and Gianfrani, L.: Advances in laser-based isotope ratio measurements: selected applications, Appl. Phys. B, 92, 439–449, https://doi.org/10.1007/s00340-008-3128-x, 2008.

Kuster, T. M., Arend, M., Bleuler, P., Günthardt-Goerg, M. S., and Schulin, R.: Water regime and growth of young oak stands subjected to air-warming and drought on two different forest soils in a model ecosystem experiment, Plant Biol., 15, 138–147, https://doi.org/10.1111/j.1438-8677.2011.00552.x, 2013.

Kuzyakov, Y.: Sources of $CO_2$ efflux from soil and review of partitioning methods, Soil Biol. Biochem., 38, 425–448, https://doi.org/10.1016/j.soilbio.2005.08.020, 2006.

Levin, I., Graul, R., and Trivett, N. B. A.: Long-term observations of atmospheric $CO_2$ and carbon isotopes at continental sites in Germany, Tellus B, 47, 23–34, https://doi.org/10.1034/j.1600-0889.47.issue1.4.x, 1995.

Maier, M. and Schack-Kirchner, H.: Using the gradient method to determine soil gas flux: A review, Agr. Forest. Meteorol., 192–193, 78–95, https://doi.org/10.1016/j.agrformet.2014.03.006, 2014.

Mortazavi, B., Prater, J. L., and Chanton, J. P.: A field-based method for simultaneous measurements of the $\delta^{18}O$ and $\delta^{13}C$ of soil $CO_2$ efflux, Biogeosciences, 1, 1–9, https://doi.org/10.5194/bg-1-1-2004, 2004.

Nelson, D. D., McManus, J. B., Herndon, S. C., Zahniser, M. S., Tuzson, B., and Emmenegger, L.: New method for isotopic ratio measurements of atmospheric carbon dioxide using a 4.3 µm pulsed quantum cascade laser, Appl. Phys. B, 90, 301–309, https://doi.org/10.1007/s00340-007-2894-1, 2008.

Oerter, E. J. and Amundson, R.: Climate controls on spatial and temporal variations in the formation of pedogenic carbonate in the western Great Basin of North America, Geol. Soc. Am. Bull., 128, 1095–1104, https://doi.org/10.1130/B31367.1, 2016.

Ohlsson, K., Singh, B., Holm, S., Nordgren, A., Lovdahl, L., and Hogberg, P.: Uncertainties in static closed chamber measurements of the carbon isotopic ratio of soil-respired CO, Soil Biol. Biochem., 37, 2273–2276, https://doi.org/10.1016/j.soilbio.2005.03.023, 2005.

O'Keefe, A. and Deacon, D. A. G.: Cavity ring-down optical spectrometer for absorption measurements using pulsed laser sources, Rev. Sci. Instrum., 59, 2544–2551, https://doi.org/10.1063/1.1139895, 1988.

O'Keefe, A., Scherer, J. J., and Paul, J. B.: Cw Integrated Cavity Output Spectroscopy, Publ. Chem. Phys. Lett., 307, 343–349, 1999.

Parameswaran, K. R., Rosen, D. I., Allen, M. G., Ganz, A. M., and Risby, T. H.: Off-axis integrated cavity output spectroscopy with a mid-infrared interband cascade laser for real-time breath ethane measurements, Appl. Optics, 48, B73-79, https://doi.org/10.1364/AO.48.000B73, 2009.

Parent, F., Plain, C., Epron, D., Maier, M., and Longdoz, B.: A new method for continuously measuring the $\delta^{13}C$ of soil $CO_2$ concentrations at different depths by laser spectrometry, Eur. J. Soil Sci., 64, 516–525, https://doi.org/10.1111/ejss.12047, 2013.

Peltola, J., Vainio, M., Ulvila, V., Siltanen, M., Metsälä, M., and Halonen, L.: Off-axis re-entrant cavity ring-down spectroscopy with a mid-infrared continuous-wave optical parametric oscillator, Appl. Phys. B, 107, 839–847, https://doi.org/10.1007/s00340-012-5074-x, 2012.

Plestenjak, G., Eler, K., Vodnik, D., Ferlan, M., Čater, M., Kanduč, T., Simončič, P., and Ogrinc, N.: Sources of soil $CO_2$ in calcareous grassland with woody plant encroachment, J. Soils Sediments, 12, 1327–1338, https://doi.org/10.1007/s11368-012-0564-3, 2012.

Ramnarine, R., Wagner-Riddle, C., Dunfield, K. E., and Voroney, R. P.: Contributions of carbonates to soil $CO_2$ emissions, Can. J. Soil Sci., 92, 599–607, https://doi.org/10.4141/cjss2011-025, 2012.

Risk, D. and Kellman, L.: Isotopic fractionation in non-equilibrium diffusive environments, Geophys. Res. Lett., 35, L02403, https://doi.org/10.1029/2007GL032374, 2008.

Satakhun, D., Gay, F., Chairungsee, N., Kasemsap, P., Chantuma, P., Thanisawanyangkura, S., Thaler, P., and Epron, D.: Soil $CO_2$ efflux and soil carbon balance of a tropical rubber plantation, Ecol. Res., 28, 969–979, https://doi.org/10.1007/s11284-013-1079-0, 2013.

Schär, C., Vidale, P. L., Lüthi, D., Frei, C., Häberli, C., Liniger, M. A., and Appenzeller, C.: The role of increasing temperature variability in European summer heatwaves, Nature, 427, 332–336, https://doi.org/10.1038/nature02300, 2004.

Schindlbacher, A., Borken, W., Djukic, I., Brandstätter, C., Spötl, C., and Wanek, W.: Contribution of carbonate weathering to the $CO_2$ efflux from temperate forest soils, Biogeochemistry, 124, 273–290, https://doi.org/10.1007/s10533-015-0097-0, 2015.

Schmidt, M. W. I., Torn, M. S., Abiven, S., Dittmar, T., Guggenberger, G., Janssens, I. A., Kleber, M., Kögel-Knabner, I., Lehmann, J., Manning, D. A. C., Nannipieri, P., Rasse, D. P., Weiner, S., and Trumbore, S. E.: Persistence of soil organic matter as an ecosystem property, Nature, 478, 49–56, https://doi.org/10.1038/nature10386, 2011.

Schönwitz, R., Stichler, W., and Ziegler, H.: $\delta^{13}C$ values of $CO_2$ from soil respiration on sites with crops of $C_3$ and $C_4$ type of photosynthesis, Oecologia, 69, 305–308, https://doi.org/10.1007/BF00377638, 1986.

Serrano-Ortiz, P., Roland, M., Sanchez-Moral, S., Janssens, I. A., Domingo, F., Goddéris, Y., and Kowalski, A. S.: Hidden, abiotic $CO_2$ flows and gaseous reservoirs in the terrestrial carbon cycle: Review and perspectives, Agr. Forest. Meteorol., 150, 321–329, https://doi.org/10.1016/j.agrformet.2010.01.002, 2010.

Sperber, C. Von, Weiler, M., and Büggemann, N.: The effect of soil moisture, soil particle size, litter layer and carbonic anhydrase on the oxygen isotopic composition of soil-released $CO_2$, Eur. J. Soil Sci., 66, 566–576, https://doi.org/10.1111/ejss.12241, 2015.

Stevenson, B. A. and Verburg, P. S. J.: Effluxed $CO_2$-13C from sterilized and unsterilized treatments of a calcareous soil, Soil Biol. Biochem., 38, 1727–1733, https://doi.org/10.1016/j.soilbio.2005.11.028, 2006.

Stumpp, C., Brüggemann, N., and Wingate, L.: Stable Isotope Approaches in Vadose Zone Research, Vadose Zone J., 17, 0, https://doi.org/10.2136/vzj2018.05.0096, 2018.

Sturm, P., Eugster, W., and Knohl, A.: Eddy covariance measurements of $CO_2$ isotopologues with a quantum cascade laser absorption spectrometer, Agr. Forest. Meteorol., 152, 73–82, https://doi.org/10.1016/j.agrformet.2011.09.007, 2012.

Tamir, G., Shenker, M., Heller, H., Bloom, P. R., Fine, P., and Bar-Tal, A.: Can Soil Carbonate Dissolution Lead to Overestimation of Soil Respiration?, Soil Sci. Soc. Am. J., 75, 1414, https://doi.org/10.2136/sssaj2010.0396, 2011.

Torn, M. S., Davis, S., Bird, J. A., Shaw, M. R., and Conrad, M. E.: Automated analysis of $^{13}C/^{12}C$ ratios in $CO_2$ and dissolved inorganic carbon for ecological and environmental applications, Rapid Commun. Mass Sp., 17, 2675–2682, https://doi.org/10.1002/rcm.1246, 2003.

von Basum, G., Halmer, D., Hering, P., Mürtz, M., Schiller, S., Müller, F., Popp, A., and Kühnemann, F.: Parts per trillion sensitivity for ethane in air with an optical parametric oscillator cavity leak-out spectrometer, Opt. Lett., 29, 797–799, https://doi.org/10.1364/OL.29.000797, 2004.

Werner, C. and Gessler, A.: Diel variations in the carbon isotope composition of respired $CO_2$ and associated carbon sources: a review of dynamics and mechanisms, Biogeosciences, 8, 2437–2459, https://doi.org/10.5194/bg-8-2437-2011, 2011.

Werner, C., Schnyder, H., Cuntz, M., Keitel, C., Zeeman, M. J., Dawson, T. E., Badeck, F.-W., Brugnoli, E., Ghashghaie, J., Grams, T. E. E., Kayler, Z. E., Lakatos, M., Lee, X., Máguas, C., Ogée, J., Rascher, K. G., Siegwolf, R. T. W., Unger, S., Welker, J., Wingate, L., and Gessler, A.: Progress and challenges in using stable isotopes to trace plant carbon and water relations across scales, Biogeosciences, 9, 3083–3111, https://doi.org/10.5194/bg-9-3083-2012, 2012.

Wingate, L., Ogée, J., Cuntz, M., Genty, B., Reiter, I., Seibt, U., Yakir, D., Maseyk, K., Pendall, E. G., Barbour, M. M., Mortazavi, B., Burlett, R., Peylin, P., Miller, J., Mencuccini, M., Shim, J. H., Hunt, J., and Grace, J.: The impact of soil microorganisms on the global budget of $\delta^{18}O$ in atmospheric $CO_2$, P. Natl. Acad. Sci. USA, 106, 22411–22415, https://doi.org/10.1073/pnas.0905210106, 2009.

Wingate, L., Ogée, J., Burlett, R., Bosc, A., Devaux, M., Grace, J., Loustau, D., and Gessler, A.: Photosynthetic carbon isotope discrimination and its relationship to the carbon isotope signals of stem, soil and ecosystem respiration, New Phytol., 188, 576–589, https://doi.org/10.1111/j.1469-8137.2010.03384.x, 2010.

Yamaoka, K., Nakagawa, T., and Uno, T.: Application of Akaike's information criterion (AIC) in the evaluation of linear pharmacokinetic equations, J. Pharmacokinet. Biopharm., 6, 165–175, https://doi.org/10.1007/BF01117450, 1978.

Zamanian, K., Pustovoytov, K., and Kuzyakov, Y.: Pedogenic carbonates: Forms and formation processes, Earth-Sci. Rev., 157, 1–17, https://doi.org/10.1016/J.EARSCIREV.2016.03.003, 2016.